

Opportunistic Arraying

Clayton Okino*, Douglas Abraham*, John Baker*, Susan Finley*, Jay Gao*, Daniel Kahan*, Andrew Klesh*, Joel Krajewski*, Norman Lay*, Shan Malhotra*, Andrew O’Dea*, Kamal Oudrhiri*, Andre Tkacenko*, Zaid Towfic*, Andrew Johnstone†

*Jet Propulsion Laboratory
California Institute of Technology
4800 Oak Grove Dr.
Pasadena, CA 91109
Clayton.M.Okino@jpl.nasa.gov

†European Space Operations Center
Robert-Bosch-Str. 5
64293 Darmstadt, Germany

Abstract— This paper discusses recent activities at JPL that are focused on extending the Opportunistic Multiple Spacecraft Per Antenna (OMSPA) concept to include arraying multiple antennas. Specifically, we explore the ability to process multiple open loop recordings associated with multiple antennas and perform the appropriate alignment and combining. We focus on using the symbol stream combining technique and provide examples of performance measurements on actual spacecraft signals for MarCO A and B as well as the Mars Express.

TABLE OF CONTENTS

1. INTRODUCTION 1
 2. OVERVIEW OF ARRAYING TECHNIQUES 2
 3. OVERVIEW OF OMSPA 3
 4. SOFTWARE RECEIVER FOR OMSPA 4
 5. OPPORTUNISTIC ARRAYING APPROACH 5
 6. ARRAY PROCESSING RESULTS 6
 7. SUMMARY 8
 ACKNOWLEDGEMENTS 8
 REFERENCES 8
 BIOGRAPHY 10

1. INTRODUCTION

In November 2018, the Interior Exploration using Seismic Investigations, Geodesy and Heat Transport (InSight) lander successfully touched down on the surface of Mars. To demonstrate the concept of “bring-your-own” communications relay option, two CubeSats (i.e. MarCO A & B) flew independently alongside InSight [MarCO]. In addition to the MarCO real-time relaying of InSight telemetry viewed live over the web, open loop recordings were obtained from DSS-54, DSS-55, and DSS-63 for both MarCO A and B. We utilize these recordings to demonstrate our arraying approach.

The Jet Propulsion Laboratory (JPL) Deep Space Network (DSN) has a long history of antenna arraying dating back to the 1970’s where initial studies showed the benefits [Ulrich70, Ulrich71] and later two 26-m antenna stations and a 64-m antenna station were arrayed to receive data from Mariner 10 during the a Mercury encounter [Wilck75]

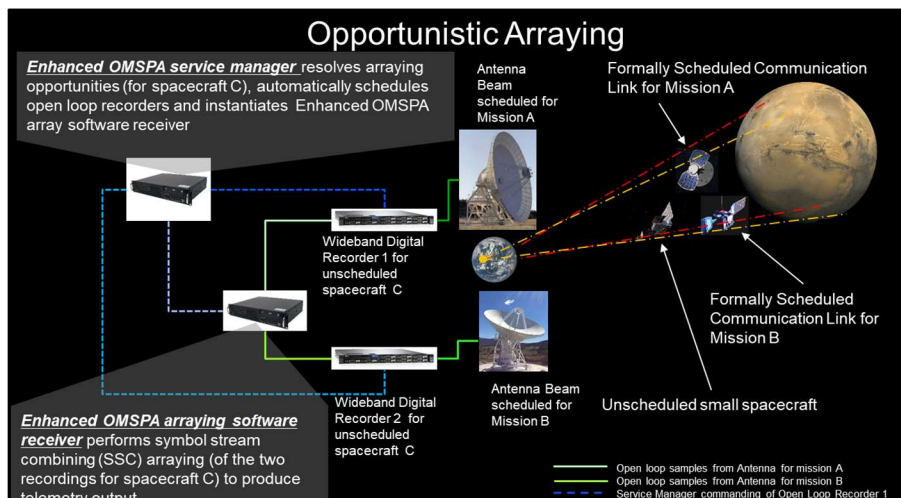


Figure 1 Opportunistic Arraying

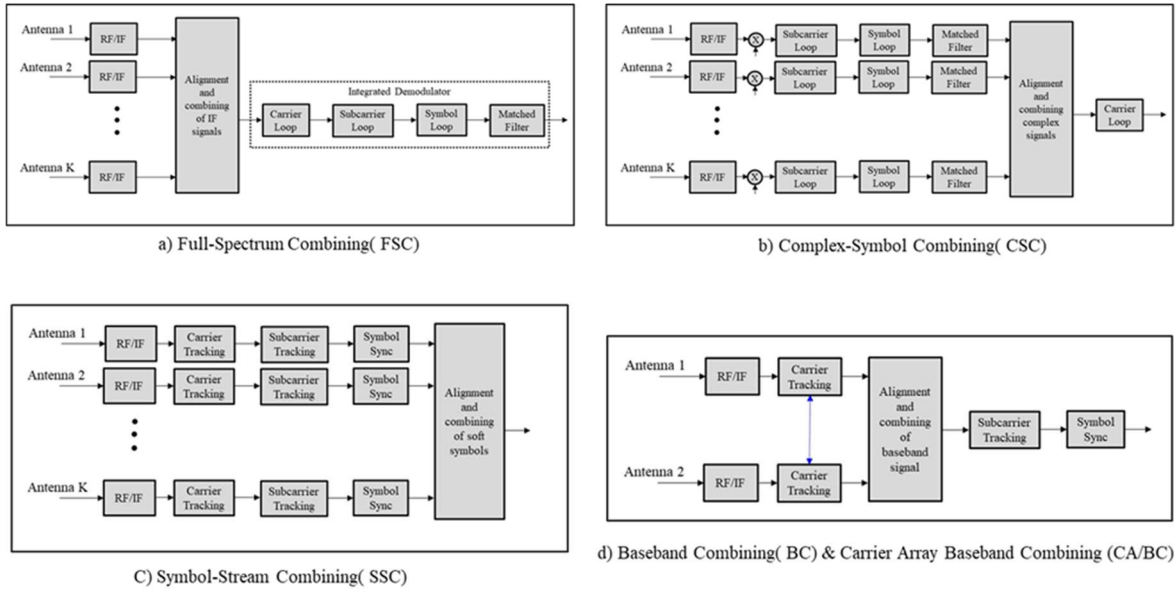


Figure 2 Block diagrams for arraying techniques

[Winkelstein75]. In 1986, Voyager 2 data received at Parkes was arrayed with the Canberra Deep Space Complex (CDSCC) [Layland85][Brown86]. This was followed by arraying for the Voyager 2 encounter at Neptune [Brown90] which included the full-spectrum combining of the Very Large Array (VLA) [Ulvestad88][Rogstad91]. Further details on the rich history and techniques on arraying with the DSN can be found in [Rogstad2003].

There are five different arraying schemes that were considered by the DSN where four of these schemes were originally captured in [Mileant91]. These five schemes [Rogstad91], are full-spectrum combining (FSC), complex-symbol combining (CSC), symbol-stream combining (SSC), baseband combining (BC), and carrier arraying (CA). Presently, the three DSN sites perform full-spectrum combining for arraying antennas. However, this approach relies on dedicating multiple antenna resources to a particular spacecraft/mission. We consider extending the Opportunistic Multiple Spacecraft Per Antenna (OMSPA) concept [Abraham2015] [Tkacenko2019] to leverage multiple antenna resources that by happenstance are pointed in the same direction (e.g. multiple missions simultaneously point antennas at Mars). By monitoring for opportunities of multiple antennas (across multiple scheduled missions) that are simultaneously within the multiple antenna beams at the same time, open loop recordings of downlink telemetry can then be array combined with a software receiver demodulator. As such, we can effectively perform opportunistic arraying without any disruption to the scheduled multiple projects/spacecraft utilizing these antennas as depicted in **Figure 1**.

There are a number of potential benefits of this Opportunistic Arraying (OA) approach relative to the traditional approach of a scheduled arraying service. First, since this is an OMSPA concept it does not require antenna scheduling. Second, the OA approach is not limited to arraying for a single spacecraft. Third, the flexibility of this form of combining, using the

open loop recordings allows for this processing to be used to perform intercontinental arraying. Furthermore, the approach allows for arraying with any antenna with a recorder that provides the correct output format. Finally, files can be reprocessed after the fact to facilitate data recovery when the spacecraft has been in an unanticipated communications configuration.

In Section 2, we provide a brief overview of the various arraying techniques. In Section 3, we provide an overview of the OMSPA strategy and in Section 4, we provide background on the software receiver used to process OMSPA open loop recorded files. In Section 5, we describe our approach to OMSPA arraying and in Section 6 we show results using open loop recorded data products from MarCO A & B as well as a Mars Express (MEX) processing example to demonstrate the opportunistic array processing approach. In Section 7, we provide some concluding remarks.

2. OVERVIEW OF ARRAYING TECHNIQUES

In Chapter 6 of [Rogstad91] five arraying schemes are presented in detail and are now briefly reviewed. As depicted in **Figure 2a**, Full-Spectrum Combining (FSC) is performed by arraying on the IF signals followed by a single demodulator that performs the carrier, subcarrier and symbol loop operations. In **Figure 2b**, Complex-Symbol Combining (CSC) involves partially demodulating down-converted signals from multiple antennas and, after combining, performing a single carrier loop demodulation. In **Figure 2c**, symbol-stream combining (SSC) involves arraying real demodulated symbols. In **Figure 2d**, baseband combining (BC) involves carrier tracking on each IF input followed by alignment and combining, then subcarrier tracking and symbol synchronization. The blue dotted line represents the addition of sharing carrier-tracking loop information to improve carrier synchronization – hence, we have, in this example, carrier arraying and baseband combining (CA/BC)

The OMSPA SM then generates the OLR recording script and downlink frequency predict file and submits these to the OLR. Finally, the OMSPA SM generates a receiver configuration file. Once the pass is completed, a copy of the OLR recording and a log file are retrieved by the OMSPA SM, and the SM executes an instantiation of the OMSPA receiver with the appropriate configuration and the OLR recording. Once the OMSPA receiver processing is complete, a copy of the telemetry file and the receiver log are provided at the portal via the OMSPA SM, and the project is notified that the data are ready. The project is then able to download the data and logs from the OMSPA portal. Clean up of files on the portal, OLR, and OMSPA receiver occurs after a pre-specified post-pass duration.

4. SOFTWARE RECEIVER FOR OMSPA

The software receiver dates back to signal analysis and demodulation tools developed under the DSN Advanced Engineering Program and various reimbursable activities. These tools originated with the concept of creating customized MATLAB signal analysis functions which are leveraged by a group of analysts [Lay2010]. An updated suite of these tools were recently utilized in a demonstration of processing Insight/MarCO downlink signals during launch [Tkacenko2019]. In preparation for an upcoming OMSPA demonstration, a generalized software receiver function was developed and is referred to as the “CCSDS_demod” depicted in **Figure 6**.

Open loop recordings in Radio Science Receiver (RSR), Wideband Very Long Baseline Interferometer (VLBI) Science Receiver (WVSR), or Open Loop Receiver (OLR) formats are accepted as input into the CCSDS_demod function.

Carrier recovery involves first obtaining a coarse frequency

estimate which is applied to the incoming I/Q baseband samples. If a subcarrier is present, the output of the coarse frequency compensation is shifted by the subcarrier frequency and then low-pass filtered to remove any residual subcarrier images. This is then followed by a forward and reverse phase-locked loop (PLL) that estimates a phase offset which is then applied as a correction to the output of the coarse frequency compensation or the subcarrier derotation/low-pass filter (if a subcarrier is present). The residual carrier phase tracking PLL also provides residual Doppler phase estimates.

The symbol timing recovery provides soft decision output symbols. In order to accomplish this, the output of the residual carrier phase tracking block is match filtered. This match filtering is multiplied with a delayed complex conjugate version of itself and then selecting the real part where the amount of delay is dependent on the pulse shaping used (i.e. Non-Return to Zero vs. Bi-Phase pulse shaping). This (timing waveform) output is band-pass filtered to obtain symbol timing instances which are then used to resample the original match filtered signal. In addition to the data stream samples, the symbol timing also provides transfer frame received times which may be used as diagnostics.

Once symbols are obtained, as depicted in **Figure 6**, there are two options for frame synchronization and decoding. In both cases, spacecraft telemetry is constructed in the form of transfer frames (TF) per the Consultative Committee for Space Data Systems (CCSDS) standards [TM2012][TM2017]. The main difference in the way TFs are formed is dependent on when the frame synchronization pattern (i.e. Attached Sync Marker) is inserted into the data stream which is dependent on turbo encoding vs convolutional coding (CC)/Reed-Solomon (RS) coding. Specifically, TFs are turbo encoded followed by adding in an Attached Sync Marker (ASM) into the data stream; where as

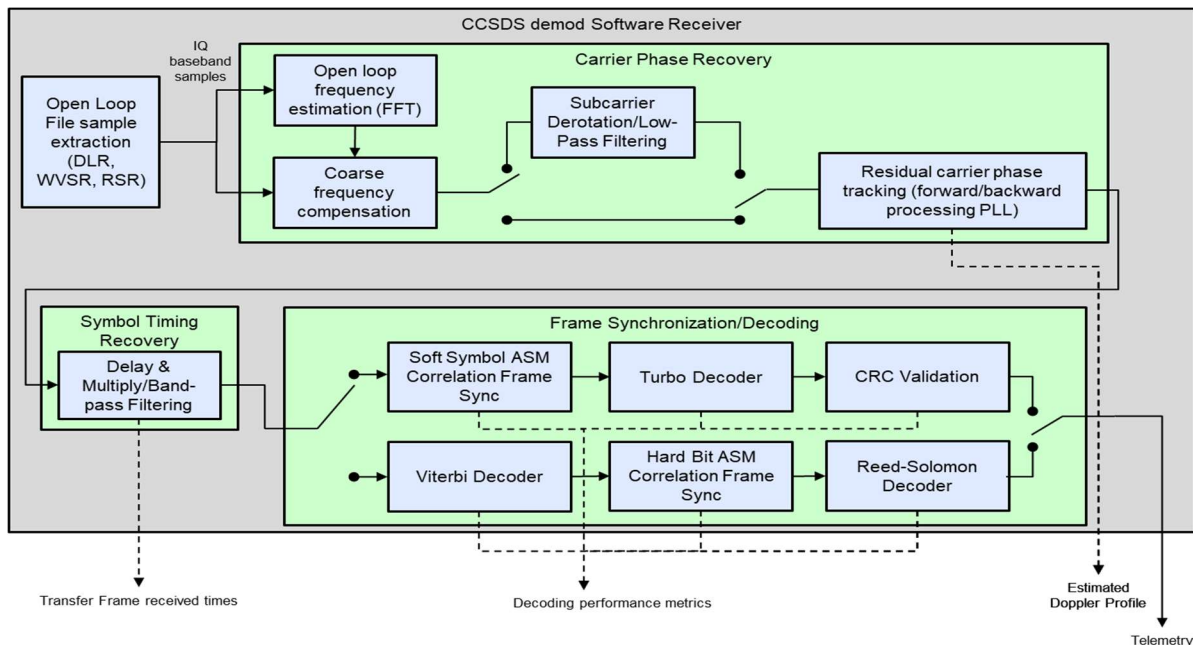


Figure 6 CCSDS_demod function version of the software receiver

for the CC/RS case, TFs are RS encoded with an ASM attached (possibly to an interleaved version of RS frames) and then CC encoded. As such, in **Figure 6**, the reverse operations occur where soft symbol synchronizations occurs for turbo encoded TFs and hard symbol synchronization occurs for CC/RS encoded TFs. For turbo encoded frames, a cyclic redundancy check (CRC) code trailer is used to validate that the TF is error free after decoding. The main outputs are these TFs which are stored in a file. In addition to the TFs, the frame synchronization and decoding block provides performance metrics from the synchronizer and decoders which may be used for diagnostics.

5. OPPORTUNISTIC ARRAYING APPROACH

As depicted in **Figure 7**, IQ broadband samples are read in from multiple open loop files (i.e. recordings from each of the antennas). Carrier phase recovery and symbol timing recovery are performed on each of these individual blocks of samples. Relative alignment and weighting estimates are computed for each of the blocks of samples and then applied to form a single soft symbol stream which is then fed into the Frame Synchronizer and Decoder.

Alignment is obtained by performing a cross-correlation against a reference sequence and finding the index of the peak:

$$\widehat{R}_{xy}(m) = \begin{cases} \sum_{n=0}^{N-m-1} x_{k,n+m} y_{k,n}^*, & m \geq 0 \\ \widehat{R}_{xy}^*(-m), & m < 0 \end{cases}$$

where

$x_{k,n}$ is the soft symbol output of the symbol tracking loop for

the k th antenna, $y_{k,n}$ represents the reference sequence where this sequence is dependent on the decoder processing path as shown in **Figure 7**, and N is the number of samples in that sequence.

For the case of the turbo decoding path, the above reference sequence is the Attached Sync Marker (ASM). For the case of the convolutional code and Reed-Solomon path, the reference sequence used is the output of the first antenna in which case the $x_{k,n}$ are for $k = 2, \dots, M$.

Once the set of symbol sequences are aligned, we combine to get the soft combined output

$$\tilde{x}_{k,n} = \sum_{k=0}^M \tilde{w}_k x_{k,n+i(k)}$$

where \tilde{w}_k is the weight estimate computed for the k th antenna, $x_{k,n+i(k)}$ are the aligned symbols for each of the k antennas, and $i(k)$ represents the shift in symbol index relative to the n th symbol for each antenna k .

From [Vilinrotter92], we utilize equation (24) which is the maximum-likelihood (ML) weight estimator as

$$\tilde{w}_k = \frac{\tilde{A}_k}{\sigma_k^2}$$

where \tilde{A}_k is the signal amplitude estimate and σ_k^2 is the noise estimate for the k th antenna. In order to obtain both of these estimates, a reference sequence is used. The noise estimate can then be computed as

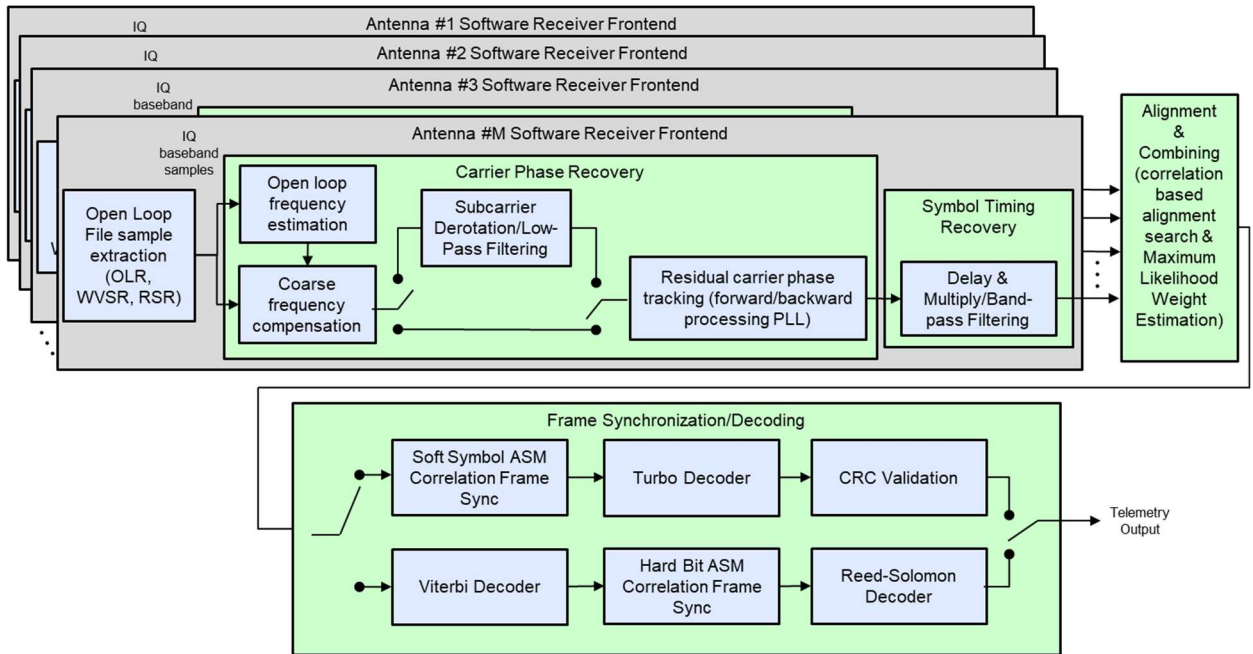


Figure 7 OMSPA Symbol Stream Combining Arraying Block Diagram

$$\sigma_k^2 = \sum_{j=0}^{\tilde{N}} (x_{k,n(k)+j} - \tilde{A}_k x_{r,k,j})^2$$

where $x_{r,k,j}$ is the j th element of the reference sequence used for the ML weight estimator and $n(k)$ represents the sample index associated with the beginning of the sequence that is being compared. Similar to the alignment procedure, the case of the turbo decoding path can use the ASM as the reference sequence; and, hence, the $n(k)$ represents the first symbol index where the ASM was detected for the k th antenna. For the case of the convolutional code and Reed-Solomon path, the reference sequence x_r can utilize the hard decision representation of each output of the symbol tracking loop since the ASMs are encoded inside the codeword of the convolutional code, and inaccessible before the decoder.

We compute the symbol Signal to Noise Ratio (SNR) as our metric to compare arraying to single antenna results. By re-encoding the output of the decoder (Turbo or Viterbi) and then using this as our reference sequence, we can then calculate the symbol SNR for the k th antenna as

$$SNR_k = \frac{\tilde{A}_k^2}{\sigma_k^2}$$

An equivalent calculation is also performed for the arrayed signal (ignoring the k subscript).

6. ARRAY PROCESSING RESULTS

In this section, we look at array processing results for the MarCO and MEX spacecraft. Between these two missions, array processing for both decoder paths are exercised. For each of the cases, we consider combining two antennas. We first consider combining signals from two antennas with the same diameter. Since the antennas are of equal size, we anticipate that performance gains would be in the region of ~ 3 dB.

Arraying MarCO A on DSS-55 and DSS-54

DSS-55 (Madrid) and DSS-54 (Madrid) antennas were arrayed using the SSC technique. SNR values were computed over a small segment of the signal for DSS-55 (Blue), DSS-54 (Green), and the SSC Arrayed Signal (black) depicted in **Figure 8**. We observe that the gain relative to the stronger signal (Green) is 2.7 dB. Using the output SNRs for each of the individual antenna, we compute a mean expected SNR for the array to be -1.01 dB where the actual SSC mean arrayed SNR is -1.05 dB which is slightly less.

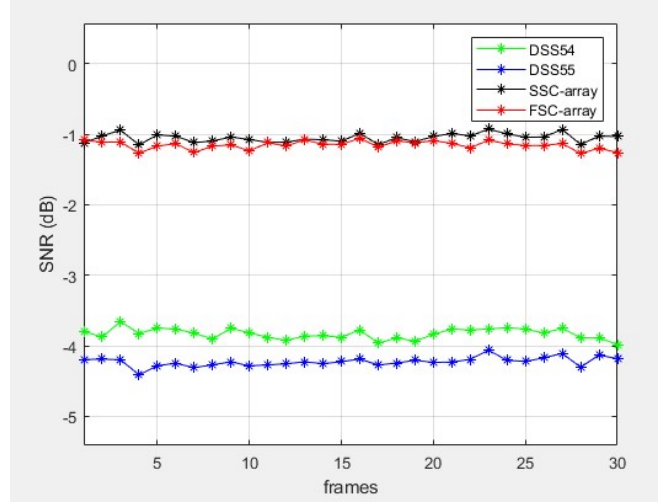


Figure 8 MarCO A SNR comparison to arraying

Recall that the FSC approach as shown in **Figure 3**, utilizes delay predicts and executes a phase difference predicts relative to the spacecraft being tracked. For this particular data collection, delay predicts were based on the InSight spacecraft while the OLR output of the MarCO A signal was what was actually recorded. We processed the FSC arrayed signal (Red) for MarCO A which showed a similar gain of 2.7 dB.

To gather a sense of the difference in delay predicts between InSight and MarCO A, a time difference predict was computed between InSight and the two receive antennas and similarly for MarCO A and the two receive antennas. The instantaneous difference between these two differences is captured in **Figure 9**, showing numbers on the order of $1\mu s$, which is an order of magnitude less than the symbol time interval.

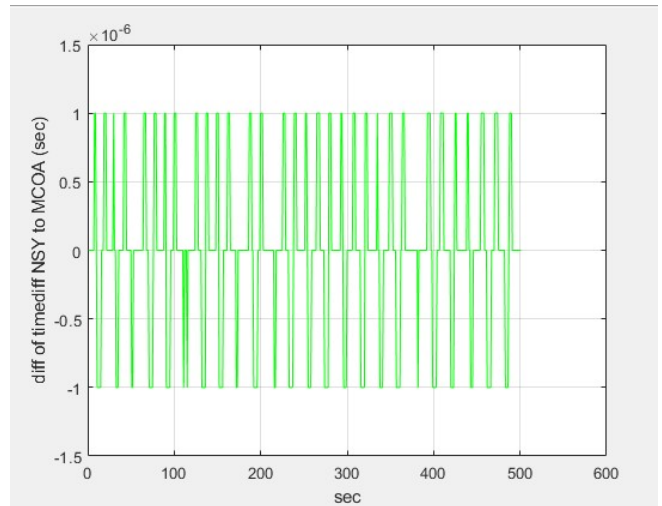


Figure 9 Time difference predicts between InSight and MarCO A relative to two antennas

We perform a similar calculation using Doppler predicts where we difference the Doppler between InSight and each of

the ground stations and similar MarCO A and each of the ground stations. We then compare the difference between these two calculations resulting in a difference of the Doppler predict differences as depicted in **Figure 10** where the maximum offset is - 0.011 Hz and results in a predicted power loss of ~ 0.01 dB.

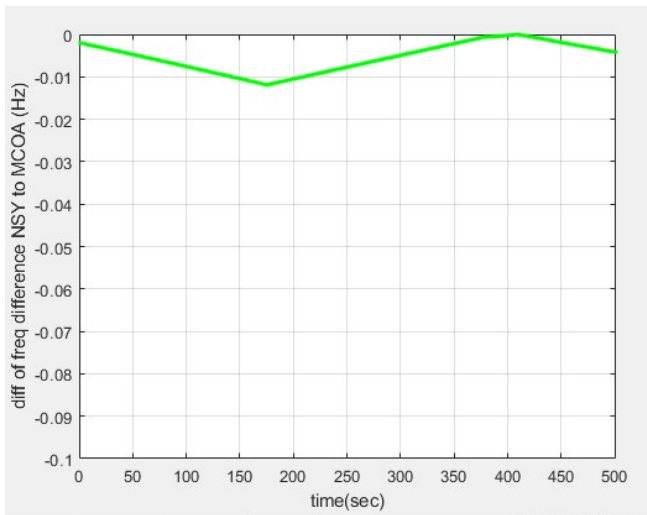


Figure 10 Doppler difference predicts between Insight and MarCO A relative to two antennas

Arraying for MarCO B on DSS-55 and DSS-54

DSS-55 and DSS-54 antennas were arrayed using the SSC technique.

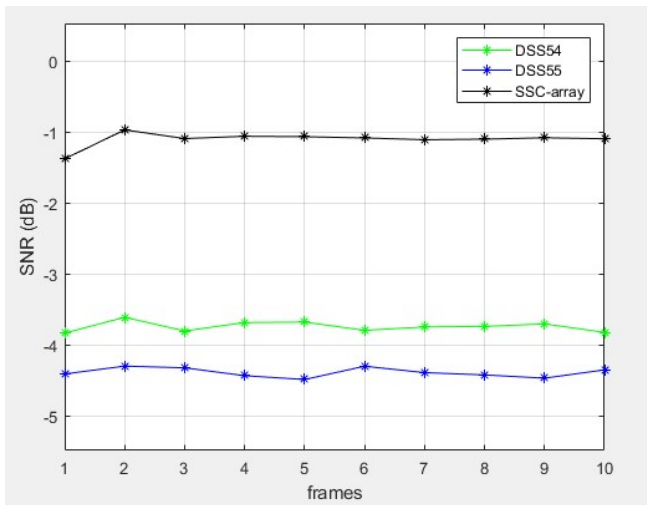


Figure 11 MarCO B SNR comparison to arraying

SNR values were computed over a small segment of the signal for DSS-55 (Blue), DSS-54 (Green), and the SSC Arrayed Signal (black) depicted in **Figure 11**. We observe that the gain relative to the stronger signal (Green) is 2.6 dB. Using the output SNRs for each of the individual antenna, we compute a mean expected SNR for the array to be -1.04 dB where the actual SSC mean arrayed SNR is -1.1 dB which is 0.07 dB less. Unfortunately, we were not able to obtain an

open loop recording for MarCO B for the FSC array.

As part of the OMSPA activities, a prototype system which included the OMSPA portal and Service Manager was developed and tested to execute antenna and link opportunities, and automatically configure the OLR and OMSPA receiver, as well as manage the file handling for all this processing. For these tests, coordination with the MEX project included obtaining pass opportunities and spacecraft setup such that the SM could then resolve potential test times. Single antenna processing was performed on a number of MEX opportunities. In addition, for one of these test opportunities, data was collected at DSS-43, DSS-36 and DSS-25. We now present some arraying results associated with these OLR recordings.

Arraying for MEX on DSS-36 and DSS-25

For the MEX telemetry, open loop recordings were obtained from DSS-36 (Canberra) and DSS-25 (Goldstone). As such, this is an example of intercontinental arraying. SNR values were computed over a small segment of the signal for DSS-36 (Green), DSS-25 (Blue), and the SSC Arrayed Signal (black) depicted in **Figure 12**. We observe that the gain relative to the stronger signal (Blue) is 2.8 dB. Using the output SNRs for each of the individual antenna, we compute a mean expected SNR for the array to be 9.47 dB where the actual SSC mean arrayed SNR is 9.37 dB which is slightly less.

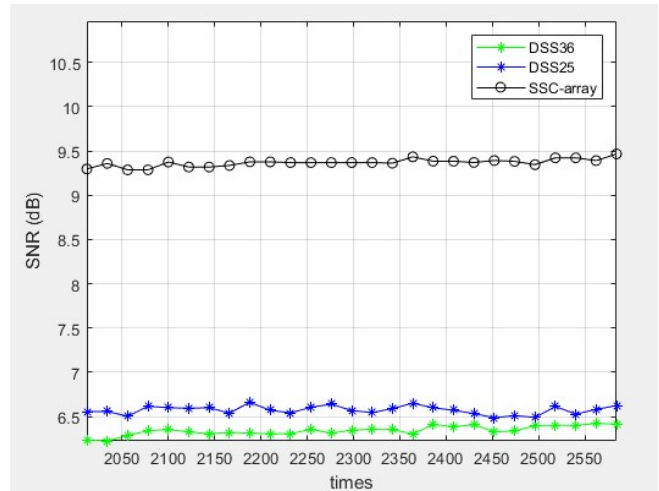


Figure 12 MEX SNR comparison to arraying

We now explore combining a 70m and a 34m. Using only these antenna diameters, we anticipate gains to be ~0.92 dB.

Arraying for MEX on DSS-43 and DSS-36

For the MEX telemetry, open loop recordings were obtained from DSS-43 and DSS-36 (both in Canberra). SNR values were computed over a small segment of the signal for DSS-43 (Green), DSS-36 (Blue), and the SSC Arrayed Signal (black) depicted in **Figure 13**. We observe that the gain relative to the stronger signal (Green) is ~0.9 dB. Using the

output SNRs for each of the individual antenna, we compute a mean expected SNR for the array to be 13.01 dB where the actual SSC mean arrayed SNR is 12.88 dB which is .13 dB less.

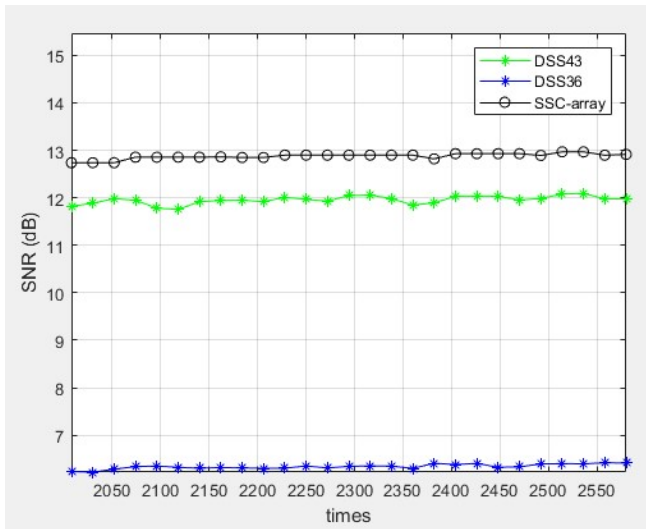


Figure 13 MEX SNR comparison 70m and 34m

Arraying for MEX on DSS-43 and DSS-25

For the MEX telemetry, open loop recordings were obtained from DSS-36 (Canberra) and DSS-25 (Goldstone). As such, this is an example of intercontinental arraying. SNR values were computed over a small segment of the signal for DSS-43 (Green), DSS-25 (Blue), and the SSC Arrayed Signal (black) depicted in **Figure 14**. We observe that the gain relative to the stronger signal (Green) is ~ 0.9 dB. Using the output SNRs for each of the individual antenna, we compute a mean expected SNR for the array to be 13.06 dB where the actual SSC mean arrayed SNR is 12.93 dB which is .13 dB less.

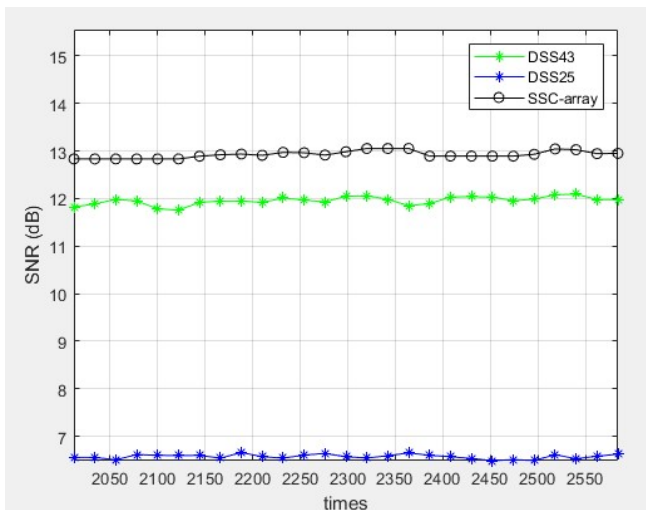


Figure 14 MEX 70m and 34m intercontinental arraying

In the correlation based approach, it was observed that,

occasionally, symbol stream misalignment occurred. Further work is needed on improving alignment robustness.

Determining performance in terms of bit error rates (BER) is challenging since we are dealing with actual spacecraft data and as such the underlying data sequences are not known a priori. Recall from [TM2012] that the waterfall plots indicate that a few tenths of a dB can easily improve BER performance by orders of magnitude (depending on the operating point for the curve). As such, our nearly 3 dB improvement due to the arraying actually resulted in significant coding performance gain. Specifically, when using the Reed-Solomon decoder, one of the output statistics is the failed codeword indicator which in all our cases resulted in zero failures implying error free performance consistent with the high SNR. For the Turbo decoder scenario, CRC checks were used and passed for all codewords also implying error free performance.

7. SUMMARY

In this paper, we described multiple well-known approaches to arraying signals from multiple antennas. We presented some refinements on the overall OMSPA approach in terms of a prototype portal and service manager which was tested on a number of MEX opportunities. We proposed a scheme for arraying in the context of the OMSPA paradigm which is referred to as Opportunistic Arraying. We developed prototype code utilizing the Symbol Stream Combining technique for performing such arraying. Using this prototype code, we demonstrated combining signals from multiple antennas on real spacecraft signals for MarCO A, MarCO B, and Mars Express – all showing gains near expected performance. Furthermore, we demonstrated intercontinental arraying.

Finally, we believe these results provide motivation for further development of the Opportunistic Arraying approach so that we can leverage features such as arraying more than a single spacecraft at one time, intercontinental arraying, and using arraying to reprocess received signals after the fact in cases of anomalous spacecraft communications conditions.

ACKNOWLEDGEMENTS

The authors thank Victor Vilmrotter on arraying discussions, the Mars Express project for enabling and supporting the collection of data processing products used in this work, and the Radio Science and Processor Systems Development groups at JPL for supporting open loop recordings for MarCO.

This work was carried out at the Jet Propulsion Laboratory, California Institute of Technology, under contract with the National Aeronautics and Space Administration.

REFERENCES

[MarCO] Mars Cube One (MarCO) Mission Overview,

<https://www.jpl.nasa.gov/cubesat/missions/MarCO.php>

[Urech70] Urech, J. M. "Telemetry Improvement Proposal for the 85-foot Antenna Network," JPL-SPS 37-63, Vol. II, 31 May 1970, pp. 116-19.

[Urech71] Urech, J. M. "Processed Data Combination for Telemetry Improvement at DSS 62," JPL Technical Report TR 32-1526, Vol. II: January and February 1971, 15 April 1971, pp. 169-76.

[Wilck75] Wilck, H. "A Signal Combiner for Antenna Arraying," DSN Progress Report PR 42-25, November and December 1974, 15 February 1975, pp. 111-17.

[Winkelstein75] Winkelstein, R. A. "Analysis of the Signal Combiner for Multiple Antenna Arraying," DSN Progress Report PR 42-26, January and December 1975, 15 April 1975, pp. 102-18.

[Layland85] Layland, J. W., and D. W. Brown. "Planning for VLA/DSN Arrayed Support to the Voyager at Neptune," TDA Progress Report PR 42-82: April-June 1985, 15 August 1985, pp. 125-35.

[Brown86] Brown, D.W., H.W. Cooper, J.W. Armstrong, and S.S. Kent, "Parkes-CDSCC Telemetry Array: Equipment Design," DSN PR 42-85, Jan-Mar 1986.

[Brown90] Brown, D. W., W. D. Brundage (National Radio Astronomy Observatory), J. S. Ulvestad, S. S. Kent, and K. P. Bartos. "Interagency Telemetry Arraying for Voyager-Neptune Encounter," TDA Progress Report PR 42-102: April-June 1990, 15 August 1990, pp. 91-118.

[Ulvestad88] Ulvestad, J.S. "Phasing the Antennas of the Very Large Array for Reception of Telemetry from Voyager 2 at Neptune Encounter," TSA Progress Report 42-94, April-June 1988.

[Rogstad91] Rogstad, D. H. "Suppressed Carrier Full-Spectrum Combining," TDA Progress Report PR 42-107: July-September 1991, 15 November 1991, pp. 12-20.

[Mileant91] Mileant, A. and S. Hinedi, "Overview of Arraying Techniques in the Deep Space Network," TDA Progress Report 42-104, February 15, 1991.

[Rogstad2003] Rogstad, D.H., A. Mileant, and T.T. Pham, "Antenna Arraying Techniques in the Deep Space Network, Monograph 5 Deep Space Communications and Navigation Series, JPL Publication 03-001, Jan 2003.

[Abraham15] Douglas S. Abraham, Susan G. Finley, David P. Heckman, Norman E. Lay, Cindy M. Lush, and Bruce E. MacNeal, "Opportunistic MSPA Demonstration #1: Final Report," IPN Progress Report 42-200 • February 15, 2015.

[Tkacenko2019] A. Tkacenko, Z. Towfic, D. Abraham, S.

Finley, S. Malhotra, A. O’dea, B. Malphrus, C. Conner, "Insight/MarCO Opportunistic Multiple Spacecraft Per Antenna (OMSPA) Demonstration," IEEE Aerospace Conference 2019, Mar 2-9, 2019, Big Sky, MT.

[Lay2010] N. Lay, M. Lyubarev, A. Tkacenko, M. Srinivasan, K. Andrews, et al., "Software Receiver Processing for Deep Space Telemetry Applications," The Interplanetary Network Progress Report, vol. 42-180, Jet Propulsion Laboratory, Pasadena, California, pp. 1–8, February 15, 2010.

[TM2012] *TM synchronization and Channel Coding – Summary of Concept and Rationale*, Green Book, Consultative Committee for Space Data Systems (CCSDS) Recommendation for Space Data Systems Standards CCSDS 130.1-G-2, Nov 2012.

[TM2017] *TM synchronization and Channel Coding – Summary of Concept and Rationale*, Blue Book, Consultative Committee for Space Data Systems (CCSDS) Recommendation for Space Data Systems Standards CCSDS 131.0-B-3, Sep. 2017.

[Vilnrotter92] V. Vilnrotter, E. Rodemich, and S. Dolinar, "Real-Time Combining of Residual Carrier Array Signals Using ML Weight Estimates," IEEE Transactions on Communications, Vol. 40.,No. 3, March 1992.

BIOGRAPHY



Clayton Okino is the technical group supervisor for the Signal Processing and Networks Group at Jet Propulsion Laboratory (JPL). He received his Ph.D. in Electrical and Computer Engineering at the University of California, San Diego. His group analyzes, develops signal processing and networking algorithms and

implements prototypes for RF and Optical Communication Systems.



Douglas Abraham is a Senior Systems Engineer within the Jet Propulsion Laboratory's Interplanetary Network Directorate (IND), which manages the Deep Space Network (DSN) and the Advanced Multi-Mission Operations System (AMMOS). For the past 20 years,

Doug has served in a variety of DSN-related capacities, most recently serving as IND's Strategic and Systems Forecasting Lead. Prior to that, Doug spent 10 years working within JPL's Mission and Systems Architecture Section, supporting the Galileo, Ulysses, and Cassini missions, as well as the Pluto Fast Flyby and "Ice and Fire" pre-formulation activities. He began his career in Reston, Virginia as a graduate student intern within the International Space Station's Program Requirements & Assessment Office. Doug graduated Magna Cum Laude from Texas A&M University in Physics (1986) and earned an M.S. in Technology and Science Policy, with specialization in technology assessment and electrical engineering, from Georgia Tech (1990).



John Baker is currently a Program Manager with nearly 30 years of experience at the Jet Propulsion Laboratory in Pasadena, California. John leads the development of planetary small spacecraft missions as well as human and robotic exploration system studies. John spent many years flying science payloads on the Space Shuttle including the Spaceborne Imaging Radar-C (SIR-C). He also spent many years working on how to reduce space mission cost from both a process as well as a technological standpoint. He was a Program Executive at NASA headquarters for the successful LRO mission to the Moon. Prior to that, he managed the Mars Science Laboratory 'Curiosity' Rover Project Systems Engineering. John has also led the development of numerous new and innovative hardware technologies, software applications and space mission concepts.



Susan Finley has been an employee of NASA's Jet Propulsion Laboratory (JPL) since January 1958, making her the longest-serving woman in NASA. Two days before Explorer 1 was launched, Finley began her career with the laboratory as a human computer, calculating rocket launch trajectories by hand. She now serves as a subsystem engineer for NASA's Deep Space Network (DSN). At JPL, she has participated in the exploration of the Moon, the Sun, all the planets, and other bodies in the Solar System.



Jay Gao joined the Jet Propulsion Laboratory in 2001 and is currently a senior researcher in the Telecommunications Research and Architecture Section. His research is primarily focused on space-based wireless communication systems, with emphasis on adaptive data rate, demand assignment multiple access,

Ka-band optimization, and Delay Tolerant Networking (DTN) for distributed, collaborative robotics applications. He is currently supporting system engineering and verification and validation activities for Europa Clipper mission's End-to-End Information System (EELS) team and had also supported Radio Science operations and data analysis for the Cassini mission. Other research interests include sensorweb, distributed communication/sensor systems, energy efficient routing and self-organization algorithm for cooperative signal processing and sensor networks. He received his Ph.D. degree in Electrical Engineering from UCLA in 2000.



Daniel Kahan is a senior member of the Planetary Radar and Radio Science Group at NASA's Jet Propulsion Laboratory. He has provided engineering support for the radio science community on multiple NASA missions including Mars Global Surveyor, Mars Reconnaissance Orbiter, the GRAIL

lunar mission, the International Cassini mission to Saturn, Mars Science Laboratory, InSight, and Juno.



Andrew Klesh is chief engineer of the MarCO mission at NASA/JPL with research interests that span deep sea, arctic, airborne, and space extreme environments. He is currently working on operational vehicles that exploit commercial technologies to maximize the exploration potential of

extreme environments. He earned his BSE Aero, BSE EE, MSE Aero, MEng Space Systems and PhD Aero from the University of Michigan, with postdoctoral fellowships on

the RAX CubeSat mission and at JAXA.



Joel Krajewski is the project manager for MarCO at the NASA Jet Propulsion Laboratory, having earned his bachelor's degree in engineering physics and master's degree in mechanical engineering, both from the University of California, Berkeley. He has worked

on many other JPL projects, including the MER rovers, Phoenix lander, Curiosity Rover, and ASTERIA.



Norman Lay is the manager of the Communications Architectures and Research Section at the NASA Jet Propulsion Laboratory. He received his PhD in Electrical Engineering from the University of Southern California. While at JPL, he has worked on a broad range of

technologies for satellite, terrestrial and deep space communications. His early work focused on the development of technologies for mobile satellite communications. He has also worked extensively on technology development for the Deep Space Network, including specialized signal analysis and detection algorithms that have been successfully utilized to support telemetry signal anomaly analysis and recovery of weak signals for missions such as Kepler and STEREO-B. Prior to joining JPL, he was employed at the General Electric Corporate Research and Development Center in Schenectady, NY.



Shan Malhotra is a Principal Engineer at NASA's Jet Propulsion Lab. He focuses on building mission critical ground data systems. For the past 20 years he has worked as a System Engineer on DSN's Service Management System – which is responsible for prediction and configuration of the systems as part of

realtime tracking. In the last 10 years he has worked as the System Engineer for the Treks – a series of Graphical Information Systems that support planetary science, mission design and public outreach for the Moon, Mars, Vesta, Titan and even Earth.



Andrew O'Dea is a ground system engineer in the Deep Space Network (DSN) Systems Engineering Group (333F) at the Jet Propulsion Laboratory.



Kamal Oudrhiri is the manager of the Planetary Radar and Radio Science Group at NASA's Jet Propulsion Laboratory and is currently the project manager of the Cold Atom Laboratory. Oudrhiri has led multi-disciplinary teams through the design, implementation and delivery of flight hardware to the radio science community. Over the last decade, Oudrhiri served in key roles on multiple NASA missions.



Andre Tkacenko received his B.S., M.S., and Ph.D. degrees in Electrical Engineering from the California Institute of Technology in 1999, 2001, and 2004, respectively. Since 2005, he has been with the Jet Propulsion Laboratory, where he is currently a signal analysis engineer in the Spectrum Engineering Group (332G).

His current work focus is in spectrum management, deep space optical communications, and software receiver design.



Zaid Towfic holds a B.S. in Electrical Engineering, Computer Science and Mathematics from the University of Iowa. He received his Electrical Engineering M.S. in 2009 and Ph.D. in 2014, both from UCLA, where he focused on signal processing, machine learning, and stochastic

optimization. After receiving his Ph. D., Zaid joined the MIT Lincoln Laboratory where he worked on distributed beam forming and geolocation, interference excision via subspace methods, simultaneous communication, and electronic warfare. Zaid joined the Jet Propulsion Laboratory in January of 2017 and has been focused on machine learning and signal processing efforts.



Andrew Johnstone has a background in Commercial Diving and Oceanography before gaining a Bachelor's degree in Aerospace Engineering from the University of Southampton. He has worked in Spacecraft Operations at ESOC in Germany for ten years, initially as a Spacecraft Controller on

XMM/INTEGRAL and MetOp-B. Currently a Spacecraft Operations Engineer on Mars Express since 2012 where his main responsibilities are with the TT&C subsystem and Mission Planning.